iScience

CellPress
OPEN ACCESS

Article

Low intensity transcranial ultrasound stimulation induces hemodynamic responses through neurovascular coupling

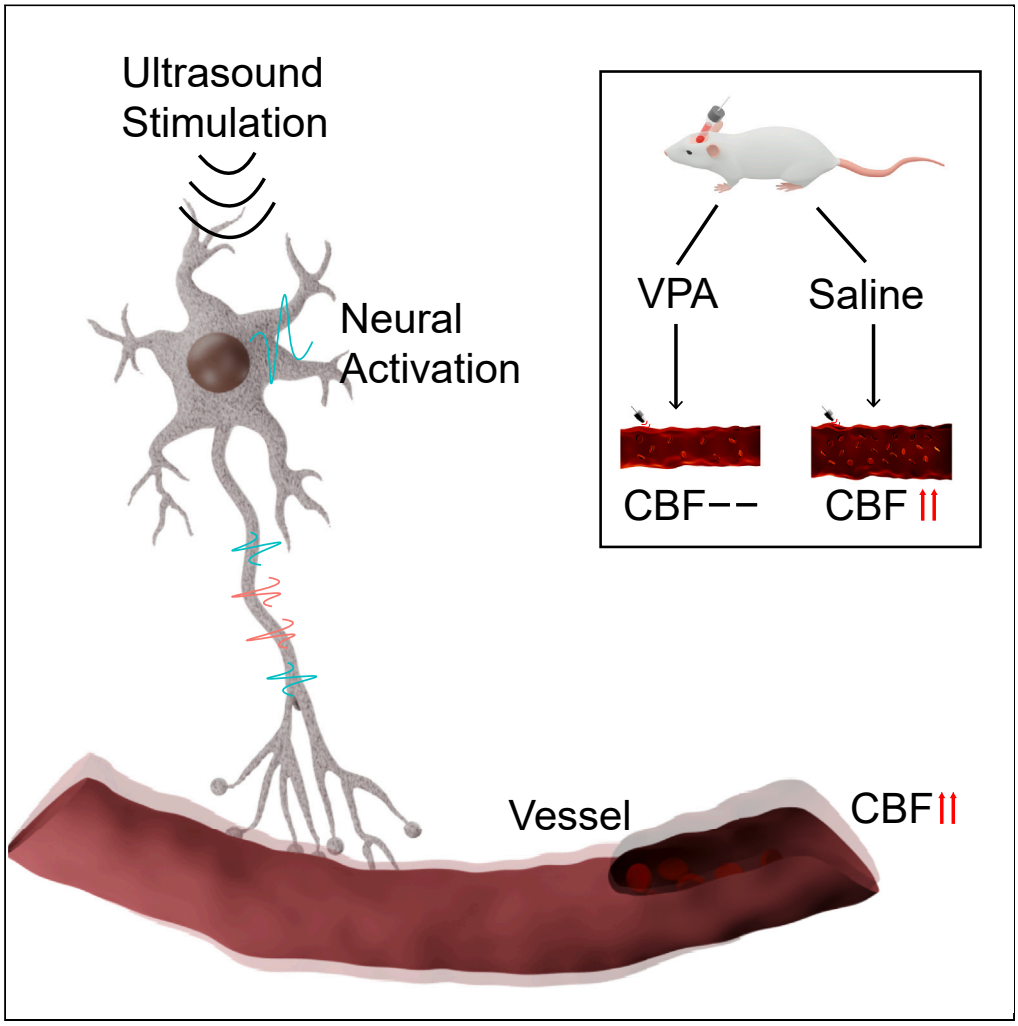

Hang Song, Ruoyu Chen, Liyuan Ren, Yinuo Zeng, Junfeng Sun, Shanbao Tong

stong@sjtu.edu.cn

Highlights

Inhibition of neural activity could weaken cerebral blood flow response to TUS

Neural inhibition altered the neurovascular coupling (NVC) under ultrasound exposure

The direct evidence for NVC pathway in hemodynamic response to TUS was observed

The changes in neural activity induced by TUS were correlated with its baseline

Song et al., iScience 27, 110269
July 19, 2024
https://doi.org/10.1016/j.isci.2024.110269

iScience

CellPress
OPEN ACCESS

Article

Low intensity transcranial ultrasound stimulation induces hemodynamic responses through neurovascular coupling

Hang Song,[1] Ruoyu Chen,[1] Liyuan Ren,[1] Yinuo Zeng,[1] Junfeng Sun,[1] and Shanbao Tong[1,2,*]

SUMMARY

Collective studies have demonstrated that transcranial ultrasound stimulation (TUS) can elicit activation in hemodynamics, implying its potential in treating cerebral or peripheral vessel-related malfunction. The theory for hemodynamic response to TUS is neurovascular coupling (NVC) following the ultrasound-induced cellular (de)polarization. However, it was not conclusive due to the co-existence of the pathway of direct ultrasound-vessel interactions. This study thus aims to investigate and provide direct evidence for NVC pathway in a rodent model of TUS by inhibiting neural activity with sodium valproate (VPA), a GABAergic agent. Twenty Sprague-Dawley rats were randomly assigned to VPA and Saline groups. Microelectrode and optical imaging were utilized to record local field potential and relative cerebral blood flow (rCBF) during baseline, before, and after TUS periods. We found the attenuated neural activity was associated with reduced rCBF responses. These results provided direct evidence for the presence of NVC pathway in hemodynamic modulation by TUS.

INTRODUCTION

Transcranial ultrasound stimulation (TUS) is an emerging non-invasive brain stimulation technique with deeper penetration and better spatial focalization than both transcranial magnetic stimulation (TMS)[1] and transcranial direct current stimulation (tDCS).[2] Cumulative studies have shown that TUS can elicit activation in electro-neurophysiological and blood flow in both animals (e.g., rat, rabbit, and macaque) and human brain.[3] Utilizing laser speckle contrast imaging (LSCI) and optical intrinsic signal imaging (OISI), recent studies observed TUS-induced enhancement of cerebral blood flow (CBF) and cerebral metabolic rate of oxygen ($CMRO_2$) in mouse cortex.[4,5] Similarly, blood-oxygen-level-dependent (BOLD) signals were found to be enhanced by TUS in human.[6,7] Our previous study also showed that TUS could induce hemodynamic enhancement and neuroprotection to ischemic stroke injury in the rat model.[8,9] These results indicated that TUS could complement existing cerebral or peripheral vessel-related malfunction therapeutics. Though TUS-induced hemodynamic results had been reported, the underlying mechanisms of hemodynamic responses to TUS were yet to be clarified.

Although the high correlation between neural and hemodynamic response to TUS was observed,[10,11] the neurovascular coupling (NVC) was not a conclusive pathway for TUS due to the co-existence of the direct interactions between ultrasound and blood vessel. *In vitro*, for example, TUS was found to promote the endothelial nitric oxide synthase (eNOS)[12] that could dilate the vessels. In animals, vasodilation by TUS had also been observed.[4] Human brachial artery diameter was reported to be increased by low-intensity ultrasound stimulation (LIUS).[13,14] Our experiments on rat's auricle also showed vasodilation in response to TUS.[15] Reports on various scales have suggested the existence of the direct ultrasound-vessel interaction, which thus makes the NVC not the sole pathway for neurovascular response to TUS. The theory of NVC in TUS, therefore, needs direct evidence.

With the aforementioned consideration, we proposed to administer sodium valproate (VPA), a GABAergic agent, before TUS to impede ion currents but enhance GABAergic inhibitory neuron activity,[16,17] and tried to confirm the NVC pathway for TUS. LSCI was implemented to measure the cortical hemodynamic responses in both VPA and Saline groups. By analyzing the main effects of *Group* and *Stage*, as well as their interactions (*Group* × *Stage*), we aimed to test the hypothesis of the existence of direct NVC pathway in TUS. Further, we explored the effect of the baseline level of neural activity on the neurovascular responses to TUS as evidence for state dependence in TUS, which had already been reported in other neuromodulations.

RESULTS

Neural activity changes induced by VPA and TUS

We first confirmed the inhibitory effect of VPA on local field potential (LFP). We looked into the two-way analysis of variance (ANOVA) of LFP power before and after VPA or saline administration in two groups before TUS (within factor of *Stage* (baseline vs. post-VPA/saline),

[1]School of Biomedical Engineering, Shanghai Jiao Tong University, Shanghai 200030, China
[2]Lead contact
*Correspondence: stong@sjtu.edu.cn
https://doi.org/10.1016/j.isci.2024.110269

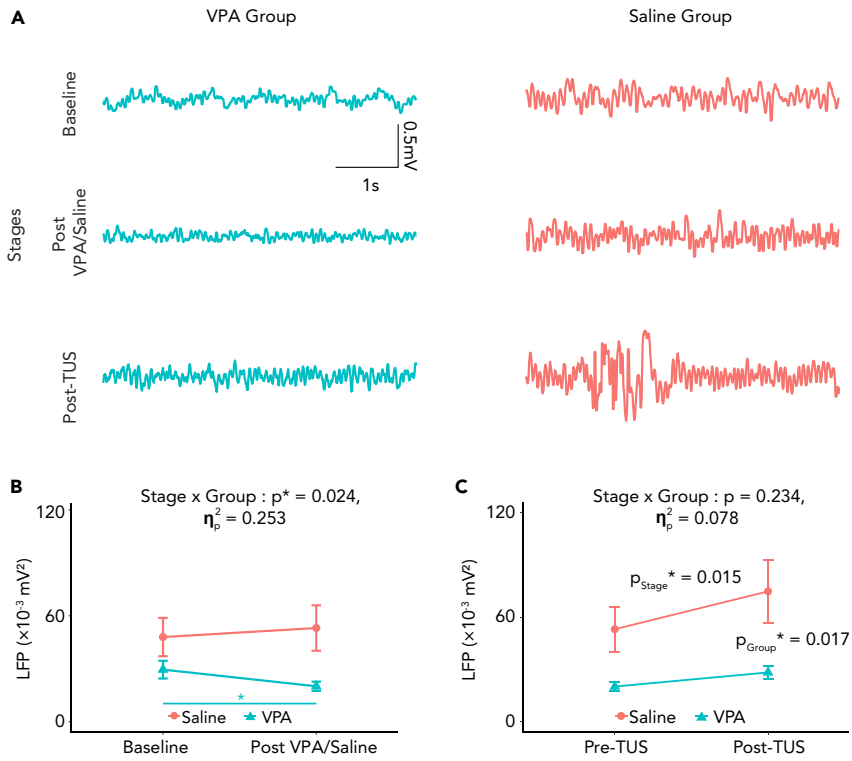

Figure 1. Neural activity responses to sodium valproate (VPA) and transcranial ultrasound stimulation (TUS), respectively

(A) Examples of acquired local field potential (LFP) signals from S1 in two groups at three *Stages*.

(B) The interaction effect of power between baseline and post-VPA/saline in two groups. The horizontal line and "*" in cyan color represent the post-hoc t tests in VPA group.

(C) The interaction effect of power between pre- and post-TUS in two groups. $p_{Group}*$ and $p_{Stage}*$ designate significant main effects ($p < 0.05$) between or within subjects. Error bars show SEM.

between factor of *Group* (VPA vs.Saline). As shown in Figure 1B, the LFP power changes in two groups were distinct, with the significant interaction effect between *Stage* and *Group* (F(1, 18) = 6.10, p = 0.024, η_p^2 = 0.253). Further post-hoc paired t test within VPA group confirmed its inhibition effect on neural activity ($LFP_{Baseline}$ = 29.49±5.03 × $10^{-3}mV^2$, $LFP_{Pre-TUS}$ = 20.06±2.61 × $10^{-3}mV^2$, t = 2.26, p = 0.036).

Further, we tested the LFP change before and after TUS in two groups (Figure 1C). Though the *Group* × *Stage* interaction was insignificant (two-way ANOVA, F(1, 18) = 1.51, p = 0.234, η_p^2 = 0.078), both main effects of between and within subjects were statistically significant(two-way ANOVA, *Stage*: F(1,18) = 7.27, p = 0.015, η_p^2 = 0.288; *Group*: F(1,18) = 6.93, p = 0.017, η_p^2 = 0.278). The significant main effect of *Stage* confirmed the TUS-induced increase of neural activity, while the significant main effect of *Group* was in line with the results in Figure 1B, demonstrating the effect of VPA. These main effects would thus imply that VPA did not completely block the neural activity induced by TUS.

Hemodynamic changes at different *stages*

We then tested the hemodynamic changes in two groups. Figure 2A showed the raw LSCI images and the mean CBF spatial distributions before and after TUS. As shown in Figure 2B, relative CBF (rCBF) declined in both groups from baseline to post-VPA/saline (Saline group: from 0.425 ± 0.60% to −2.37 ± 2.11%; VPA group: from −0.87 ± 0.80% to −8.07 ± 2.72%). Also, the main effect within subjects (*Stage*) was statistically significant (two-way ANOVA, F(1,18) = 12.33, p = 0.002, η_p^2 = 0.407). However, neither main effect of *Group* (two-way ANOVA, F(1,18) = 2.78, p = 0.113, η_p^2 = 0.134) nor the interaction effect (two-way ANOVA, F(1,18) = 2.40, p = 0.139, η_p^2 = 0.118) was significant. Thus, we could not conclude a VPA-related rCBF decline in this experiment.

Further comparison of the pre-TUS with the post-TUS rCBF levels revealed distinct responses in Saline group, whereas the VPA group only showed a weak increase in rCBF. In further quantitative analysis (shown in Figure 2C), the mean rCBF in Saline group increased from −2.37 ± 2.11% to 9.27 ± 3.45% (paired t test: t = 5.04, p = 0.00008), while VPA group displayed minimal increasing in mean rCBF (from Pre-TUS: −8.07 ± 2.72% to Post-TUS: −6.34 ± 2.13%, paired t test: t = 0.75, p = 0.463). A significant and large interaction effect (F(1,18) = 8.32, p = 0.007, η_p^2 = 0.338) was observed. The result indicated that VPA did interfere with rCBF activation in response to TUS, i.e., hemodynamic responses to TUS varied when neural activity was inhibited.

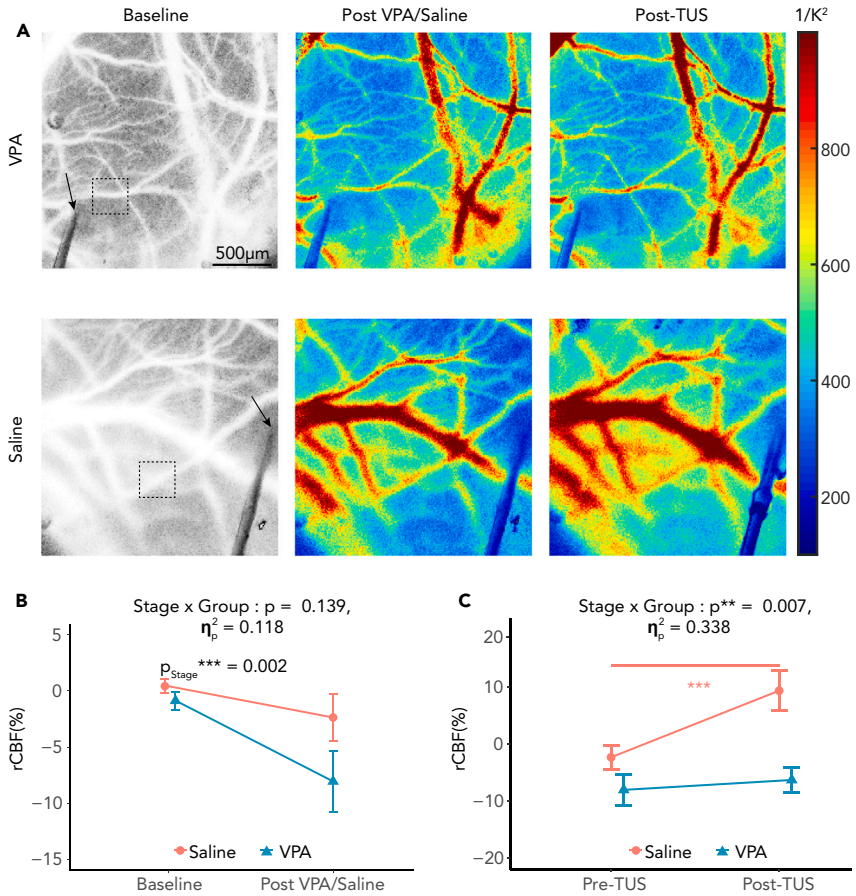

Figure 2. Hemodynamic changes at different *Stages*

(A) Examples of raw laser speckle contrast imaging (LSCI) images and pseudo-color images of cerebral blood flow (CBF). The arrow indicates the location of the microelectrode, and the dashed squares indicate the regions of interest (ROIs).

(B) The interaction effect of relative CBF (rCBF) between baseline and post-VPA/saline in two groups. p_{Stage} ∗∗ described the main effect of *Stage*.

(C) The interaction effect of rCBF between pre- and post-TUS in two groups. The horizontal line and "***" in red represent the post-hoc t test in Saline group. Error bars show standard error of the mean (SEM). "**" and "***" denotes $p < 0.01$ and $p < 0.001$, respectively.

DISCUSSION

NVC, also known as functional hyperemia, has been used to explain the change in local blood perfusion due to altered neural activity.[18] According to NVC theory, external stimuli or neural self-oscillations trigger the initial neural signaling, activating interneurons and neurotransmitters release that cause vasodilation and then CBF increases.[19] TUS has recently been regarded as an emerging technique for neuromodulation with great potential for clinical applications. The underlying mechanisms of TUS, however, are under debate. The neural intramembrane cavitation excitation (NICE) model[20] has been proposed as one of the possible mechanisms. According to the NICE model, ultrasound-induced changes in neuron membrane thickness alter the membrane capacitance, thereby changing the action potential discharge threshold. This TUS-induced alteration of neurons would be reflected as the enhancement of neural activity.[3] Combined with the NVC theory, it is a rational hypothesis that the locally raised CBF level meets the activated neural level evoked by TUS, i.e., NVC is a pathway for TUS-induced hemodynamic activation. However, due to the co-existence of the direct ultrasound-vessel interaction,[13–15] the NVC pathway needs to be confirmed by direct evidence. In this study, we thus pursued to verify the existence of the pathway of NVC in TUS-induced CBF changes. Neither neural activities nor ultrasound-induced mechanical effects could be completely blocked, even with the administration of neural inhibitory VPA. Thus, though many researchers have reported TUS-induced CBF activation, the role of NVC in TUS still lacks direct evidence. By investigating the interaction effects of *Group*×*Stage* on LFP power as well as the rCBF, we were able to confirm VPA effect from baseline to post-VPA/saline and distinct TUS-induced effect from pre-TUS to post-TUS.

VPA is typically administered orally or via an intraperitoneal injection, and it generally takes about 10 min to take effect.[21] This delay could potentially prolong the duration of the experiment. Conversely, tetrodotoxin (TTX), a sodium channel blocker, is delivered through an intracisternal injection to inhibit transcranial ultrasound stimulation (TUS).[22] The key distinction between VPA and TTX lies in their mechanisms of

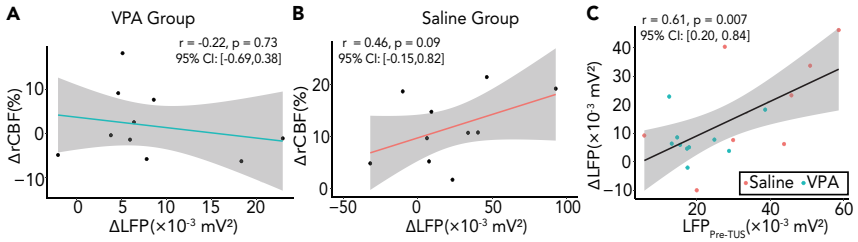

Figure 3. Correlations between the relative cerebral blood flow (rCBF) change and the local field potential (LFP) change under ultrasound exposure

(A) Pearson's correlation between the rCBF change and the LFP power change in VPA group.

(B) Pearson's correlation between the CBF and LFP change in Saline group.

(C) Pearson's correlation between $LFP_{pre-TUS}$ and Δ LFP ($LFP_{post-TUS}$ - $LFP_{pre-TUS}$). The lines and the shadows represented the linear regressions and the 95% confidence bands, respectively.

action. VPA enhances the activity of GABAergic neurons, whereas TTX obstructs sodium channels.[23] As such, TTX is more suitable for research focused on ion channels. Nevertheless, TTX's toxicity and safety concerns, combined with the specialized training required for its administration, make it less accessible.[24,25]

The LFP results showed that VPA effectively inhibited the cortical neural activation (Figure 1B). Nonetheless, VPA could not completely block the TUS-induced LFP enhancement as we found a significant increase of LFP power after TUS in either VPA or Saline group (Figure 1C).

Meanwhile, we found that VPA could also significantly lower the rCBF. The most interesting result in our experiment is a significant interaction effect *Group*×*Stage* on rCBF (Figure 2C), indicating distinct TUS-induced rCBF activation in VPA and Saline groups, with a considerable effect size ($\eta_p^2 = 0.338$). Combining with the LFP results, we concluded that TUS successfully induced neural activation and then rCBF activation through NVC, regardless of the direct ultrasound-vessel interaction. However, we also noted that the results in this experiment could not be used to infer whether the direct ultrasound-vessel pathway exists as we could not completely block the TUS-induced neural activation (Figure 1C).

Besides, for the correlation between the rCBF change and the LFP power change in both groups (Figures 3A and 3B), notably, we can observe a weak and statistically non-significant correlation between ΔLFP (i.e., $LFP_{post-TUS}$-$LFP_{pre-TUS}$) and $\Delta rCBF$ (i.e., $rCBF_{post-TUS} - rCBF_{pre-TUS}$) in VPA group (Pearson's $r(8) = -0.22$, $p = 0.73, 95\%\ CI: [-0.69, 0.38]$). However, the very likely existence of a medium or high level of positive correlation remained in Saline group (Pearson's $r(8) = 0.46, p = 0.09, 95\%\ CI: [-0.15, 0.82]$). The correlations did not reach statistical significance because the sample size in this study, determined by interaction effect, was unplanned for the correlation test. However, the correlation of neurovascular response to TUS in Saline group was in concert with previous studies.[10,11] The correlation between neurovascular changes in Saline group was consistent with Figure 2C, supporting the NVC pathway for TUS.

In other neuromodulation modalities, researchers have reported an interesting phenomenon of state-dependent neuromodulation effect.[26,27] In tDCS and TMS, studies have shown that the baseline states (sleep, anesthesia, or awake) were associated with effects of the modulation.[28–30] Researchers have also observed that the baseline neural activation could profoundly affect the outcome of TUS.[31] In the present study, the distinct TUS-induced enhancement (Figures 1C and 2C) in VPA and Saline groups could also be interpreted as the state dependency of TUS. For example, the LFP power activation before and after TUS in two groups were significantly different (Saline group: $LFP_{pre-TUS} = 53.07 \pm 12.88 \times 10^{-3} mV^2$, $LFP_{post-TUS} = 74.83 \pm 12.22 \times 10^{-3} mV^2$, t = 2.78, $p = 0.012$; VPA group: $LFP_{pre-TUS} = 20.06 \pm 2.61 \times 10^{-3} mV^2$, $LFP_{post-TUS} = 28.18 \pm 3.79 \times 10^{-3} mV^2$, $t = 1.04$, $p = 0.314$). Further, we did a correlation analysis between Pre-TUS and $\Delta LFP(LFP_{post-TUS} - LFP_{pre-TUS})$ (Figure 3C). As the LFP power was not normally distributed (Shapiro-Wilk test: $p = 0.017$), we calculated the Pearson's correlation coefficient r between LFP power before and after TUS among all subjects in two groups by discarding two outliers(Cook's D > 4/20 = 0.2).[32] As shown in Figure 3C, the neural response had a positive correlation with the state before TUS ($r(16) = 0.61$, $p = 0.007$, $95\%CI: [0.20, 0.84]$). These results enriched the evidences for state-dependent neuromodulations.[31,33,34] Nonetheless, we, however, did not find a similar state-dependent effect on rCBF response ($r(16) = -0.16$, $p = 0.522$, $95\%CI: [-0.58, 0.33]$). In clinical practice, such a state-dependent TUS could complicate its applications as some subjects may not respond as expected.

Limitations of the study

There are several limitations to the present study. First, the parameters of TUS play a vital role in the effects on hemodynamic responses. It is unknown whether the performance of NVC pathway would alter under different parameters of TUS. Second, we did not combine the results of rCBF with other measurements of vessel diameters (e.g., two-photon fluorescence imaging). These measurements may provide mechanistic insights into vessels following TUS. Last, the finding at the motor cortex may not be generalized to other cortical regions. More researches are required to prove the NVC pathway of TUS in rats.

In summary, by applying TUS to S1 of rats and comparing the neural and hemodynamic changes in both VPA and Saline groups, we presented direct evidence for the NVC pathway for TUS. The results also confirmed the existence of a state-dependent response to TUS.

STAR★METHODS

Detailed methods are provided in the online version of this paper and include the following:

- KEY RESOURCES TABLE
- RESOURCE AVAILABILITY
  - Lead contact
  - Materials availability
  - Data and code availability
- EXPERIMENTAL MODEL AND STUDY PARTICIPANT DETAILS
- METHOD DETAILS
  - Experimental protocols
  - TUS parameters
  - Sodium valproate (VPA)
  - LFP-LSCI recordings
  - Image and data processing
- QUANTIFICATION AND STATISTICAL ANALYSIS

SUPPLEMENTAL INFORMATION

Supplemental information can be found online at https://doi.org/10.1016/j.isci.2024.110269.

ACKNOWLEDGMENTS

This work was partly supported by MOST 2030 Brain Project (no. 2022ZD0208500), National Key R&D Program of China (no. 2022YFC3601200), National Natural Science Foundation of China (61876108 and 62376157), Science and Technology Cooperation Program of Shanghai Jiao Tong University in Inner Mongolia Autonomous Region (2022XYJG0001-01-21). J.S. is also partly supported by the Fundamental Research Funds for the Central Universities (YG2023QNB18).

AUTHOR CONTRIBUTIONS

H.S., J.S., and S.T. designed the experiment. H.S., R.C., Y.Z., and R.L. performed the study; S.H. analyzed the results; S.H., L.R., J.S., and S.T. wrote the paper. All authors have read and approved the final version of the manuscript.

DECLARATION OF INTERESTS

The authors declare no competing interests.

Received: December 23, 2023
Revised: April 20, 2024
Accepted: June 12, 2024
Published: June 17, 2024

REFERENCES

1. Hallett, M. (2007). Transcranial magnetic stimulation: a primer. Neuron *55*, 187–199.
2. Stagg, C.J., and Nitsche, M.A. (2011). Physiological basis of transcranial direct current stimulation. Neuroscientist *17*, 37–53.
3. Fomenko, A., Neudorfer, C., Dallapiazza, R.F., Kalia, S.K., and Lozano, A.M. (2018). Low-intensity ultrasound neuromodulation: An overview of mechanisms and emerging human applications. Brain Stimul. *11*, 1209–1217.
4. Yuan, Y., Zhao, Y., Jia, H., Liu, M., Hu, S., Li, Y., and Li, X. (2018). Cortical hemodynamic responses under focused ultrasound stimulation using real-time laser speckle contrast imaging. Front. Neurosci. *12*, 269.
5. Kim, E., Anguluan, E., and Kim, J.G. (2017). Monitoring cerebral hemodynamic change during transcranial ultrasound stimulation using optical intrinsic signal imaging. Sci. Rep. *7*, 13148.
6. Ai, L., Mueller, J.K., Grant, A., Eryaman, Y., and Legon, W. (2016). Transcranial focused ultrasound for bold fmri signal modulation in humans. In 38th Annual International Conference of the IEEE Engineering in Medicine and Biology Society (EMBC) (IEEE), pp. 1758–1761.
7. Lee, W., Kim, H.-C., Jung, Y., Chung, Y.A., Song, I.-U., Lee, J.-H., and Yoo, S.-S. (2016). Transcranial focused ultrasound stimulation of human primary visual cortex. Sci. Rep. *6*, 34026.
8. Guo, T., Li, H., Lv, Y., Lu, H., Niu, J., Sun, J., Yang, G.-Y., Ren, C., and Tong, S. (2015). Pulsed transcranial ultrasound stimulation immediately after the ischemic brain injury is neuroprotective. IEEE Trans. Biomed. Eng. *62*, 2352–2357.
9. Li, H., Sun, J., Zhang, D., Omire-Mayor, D., Lewin, P.A., and Tong, S. (2017). Low-intensity (400 mW/cm^2, 500 kHz) pulsed transcranial ultrasound preconditioning may mitigate focal cerebral ischemia in ratsmw/cm2, 500 khz) pulsed transcranial ultrasound preconditioning may mitigate focal cerebral ischemia in rats. Brain Stimul. *10*, 695–702.
10. Yuan, Y., Wang, Z., Wang, X., Yan, J., Liu, M., and Li, X. (2019). Low-intensity pulsed ultrasound stimulation induces coupling between ripple neural activity and hemodynamics in the mouse visual cortex. Cereb. Cortex *29*, 3220–3223.
11. Yuan, Y., Wang, Z., Liu, M., and Shoham, S. (2020). Cortical hemodynamic responses induced by low-intensity transcranial ultrasound stimulation of mouse cortex. Neuroimage *211*, 116597.
12. Altland, O.D., Dalecki, D., Suchkova, V.N., and Francis, C.W. (2004). Low-intensity ultrasound increases endothelial cell nitric oxide synthase activity and nitric oxide synthesis. J. Thromb. Haemost. *2*, 637–643.
13. Iida, K., Luo, H., Hagisawa, K., Akima, T., Shah, P.K., Naqvi, T.Z., and Siegel, R.J. (2006).

Noninvasive low-frequency ultrasound energy causes vasodilation in humans. J. Am. Coll. Cardiol. *48*, 532–537.
14. Hauck, M., Noronha Martins, C., Borges Moraes, M., Aikawa, P., da Silva Paulitsch, F., Méa Plentz, R.D., Teixeira da Costa, S., Vargas da Silva, A.M., and Signori, L.U. (2019). Comparison of the effects of 1 mhz and 3 mhz therapeutic ultrasound on endothelium-dependent vasodilation of humans: a randomised clinical trial. Physiotherapy *105*, 120–125.
15. Song, H., Sun, J., Miao, P., and Tong, S. (2023). Vascular response to low-intensity ultrasound stimulation. In 45th Annual International Conference of the IEEE Engineering in Medicine & Biology Society (EMBC) (IEEE), pp. 1–4.
16. VanDongen, A.M., VanErp, M.G., and Voskuyl, R.A. (1986). Valproate reduces excitability by blockage of sodium and potassium conductance. Epilepsia *27*, 177–182.
17. Judge, S.I.V., Smith, P.J., Stewart, P.E., and Bever, C.T., Jr. (2007). Potassium channel blockers and openers as cns neurologic therapeutic agents. Recent Pat. CNS Drug Discov. *2*, 200–228.
18. Pasley, B., and Freeman, R. (2008). Neurovascular coupling. Scholarpedia *3*, 5340.
19. Phillips, A.A., Chan, F.H., Zheng, M.M.Z., Krassioukov, A.V., and Ainslie, P.N. (2016). Neurovascular coupling in humans: physiology, methodological advances and clinical implications. J. Cereb. Blood Flow Metab. *36*, 647–664.
20. Plaksin, M., Shoham, S., and Kimmel, E. (2014). Intramembrane cavitation as a predictive bio-piezoelectric mechanism for ultrasonic brain stimulation. Phys. Rev. X *4*, 011004.
21. Löscher, W. (2002). Basic pharmacology of valproate: a review after 35 years of clinical usefor the treatment of epilepsy. CNS drugs *16*, 669–694.
22. Tufail, Y., Matyushov, A., Baldwin, N., Tauchmann, M.L., Georges, J., Yoshihiro, A., Tillery, S.I.H., and Tyler, W.J. (2010). Transcranial pulsed ultrasound stimulates intact brain circuits. Neuron *66*, 681–694.
23. Lorentz, M.N., Stokes, A.N., Rößler, D.C., and Lötters, S. (2016). Tetrodotoxin. Curr. Biol. *26*, R870–R872.
24. Bane, V., Lehane, M., Dikshit, M., O'Riordan, A., and Furey, A. (2014). Tetrodotoxin: Chemistry, toxicity, source, distribution and detection. Toxins *6*, 693–755.
25. Patockaa, J., and Stredab, L. (2002). Brief review of natural nonprotein neurotoxins. ASA Newslett. *89*, 16–24.
26. Marder, E., O'Leary, T., and Shruti, S. (2014). Neuromodulation of circuits with variable parameters: single neurons and small circuits reveal principles of state-dependent and robust neuromodulation. Annu. Rev. Neurosci. *37*, 329–346.
27. McCormick, D.A., Nestvogel, D.B., and He, B.J. (2020). Neuromodulation of brain state and behavior. Annu. Rev. Neurosci. *43*, 391–415.
28. Learmonth, G., Thut, G., Benwell, C.S.Y., and Harvey, M. (2015). The implications of state-dependent tdcs effects in aging: behavioural response is determined by baseline performance. Neuropsychologia *74*, 108–119.
29. Bradley, C., Nydam, A.S., Dux, P.E., and Mattingley, J.B. (2022). State-dependent effects of neural stimulation on brain function and cognition. Nat. Rev. Neurosci. *23*, 459–475.
30. Pasley, B.N., Allen, E.A., and Freeman, R.D. (2009). State-dependent variability of neuronal responses to transcranial magnetic stimulation of the visual cortex. Neuron *62*, 291–303.
31. Wang, X., Zhang, Y., Zhang, K., and Yuan, Y. (2021). Influence of behavioral state on the neuromodulatory effect of low-intensity transcranial ultrasound stimulation on hippocampal ca1 in mouse. Neuroimage *241*, 118441.
32. Krasker, W.S., Kuh, E., and Welsch, R.E. (1983). Estimation for dirty data and flawed models. Handb. Econom. *1*, 651–698.
33. Yang, P.-F., Phipps, M.A., Jonathan, S., Newton, A.T., Byun, N., Gore, J.C., Grissom, W.A., Caskey, C.F., and Chen, L.M. (2021). Bidirectional and state-dependent modulation of brain activity by transcranial focused ultrasound in non-human primates. Brain Stimul. *14*, 261–272.
34. Yang, P.-F., Phipps, M.A., Newton, A.T., Jonathan, S., Manuel, T.J., Gore, J.C., Grissom, W.A., Caskey, C.F., and Chen, L.M. (2022). Differential dose responses of transcranial focused ultrasound at brain regions indicate causal interactions. Brain Stimul. *15*, 1552–1564.
35. Charan, J., and Kantharia, N.D. (2013). How to calculate sample size in animal studies? J. Pharmacol. Pharmacother. *4*, 303–306.
36. Briers, J.D., and Webster, S. (1996). Laser speckle contrast analysis (lasca): a nonscanning, full-field technique for monitoring capillary blood flow. J. Biomed. Opt. *1*, 174–179.
37. Cheng, H., Luo, Q., Zeng, S., Chen, S., Cen, J., and Gong, H. (2003). Modified laser speckle imaging method with improved spatial resolution. J. Biomed. Opt. *8*, 559–564.
38. Miao, P., Rege, A., Li, N., Thakor, N.V., and Tong, S. (2010). High resolution cerebral blood flow imaging by registered laser speckle contrast analysis. IEEE Trans. Biomed. Eng. *57*, 1152–1157.
39. Boas, D.A., and Dunn, A.K. (2010). Laser speckle contrast imaging in biomedical optics. J. Biomed. Opt. *15*, 011109.
40. Zhang, D., Li, H., Sun, J., Hu, W., Jin, W., Li, S., and Tong, S. (2019). Antidepressant-like effect of low-intensity transcranial ultrasound stimulation. IEEE Trans. Biomed. Eng. *66*, 411–420.
41. Browne, T.R. (1980). Valproic acid. N. Engl. J. Med. *302*, 661–666.
42. Hariton, C., Ciesielski, L., Simler, S., Valli, M., Jadot, G., Gobaille, S., Mesdjian, E., and Mandel, P. (1984). Distribution of sodium valproate and gaba metabolism in cns of the rat. Biopharm. Drug Dispos. *5*, 409–414.
43. Löscher, W. (1999). Valproate: a reappraisal of its pharmacodynamic properties and mechanisms of action. Prog. Neurobiol. *58*, 31–59.
44. Wang, X., Yan, J., Wang, Z., Li, X., and Yuan, Y. (2020). Neuromodulation effects of ultrasound stimulation under different parameters on mouse motor cortex. IEEE Trans. Biomed. Eng. *67*, 291–297.

STAR★METHODS

KEY RESOURCES TABLE

REAGENT or RESOURCE	SOURCE	IDENTIFIER
Chemicals, peptides, and recombinant proteins		
Sodium valproate	Macklin	CAS: 1069-66-5
Deposited data		
Local field potential data	This manuscript	https://osf.io/6ngp5/
Relative cerebral blood flow data	This manuscript	https://osf.io/sn58w/
Software and algorithms		
Jamovi	Computer software	https://www.jamovi.org
MATLAB	Mathworks	www.mathworks.com/
Local field potential data processing code	This manuscript	https://osf.io/8rjwe/
Relative cerebral blood flow data processing code	This manuscript	https://osf.io/waupg/

RESOURCE AVAILABILITY

Lead contact

Further information and requests for resources and reagents should be directed to and will be fulfilled by the lead contact, Dr. Shanbao Tong (stong@sjtu.edu.cn).

Materials availability

This study did not generate new unique reagents.

Data and code availability

- Data: LFP power data (*LFP_Power_data.xlsx*), and relative cerebral blood flow data (*rCBF_data.xlsx*) are freely available via an open-access data-sharing repository and are publicly available as of the date of publication. Accession numbers are listed in the key resources table.
- Code: LFP data processing (*LFP_processing.m*), and relative cerebral blood flow data processing codes(*rCBF_processing.m*) are freely available via an open-access data-sharing repository and are publicly available as of the date of publication. Accession numbers are listed in the key resources table.
- Additional information: Any additional information required to reanalyze the data reported in this paper is available from the lead contact upon request.

EXPERIMENTAL MODEL AND STUDY PARTICIPANT DETAILS

Animal experiments in this study were approved by bioethics committee school of biomedical engineering Shanghai Jiao Tong University (the study approval number: 2022015). A total of 20 adult male Sprague-Dawley rats (220-320 g, Slac Laboratory Animal Co.Ltd., Shanghai, China) were equally and randomly assigned to two groups, i.e., VPA group and Saline group. The sample size was decided by power analysis based on a pilot experiment, with a type-I error $\alpha = 0.01$ and statistical power $1 - \beta = 0.80$, respectively.[35] A cranial window was prepared 6 h before the experiment. During the surgery, rats were anesthetized with isoflurane (5% initial and 2% maintenance) and secured to the stereotaxic frame. The temperature of each animal was monitored and maintained at $37 \pm 0.5^{\circ}C$ using a closed-loop temperature controller (Model: 69002, RWD., Shenzhen, China). All procedures were conducted under standard sterile precautions. After shaving, a middle incision was made on the scalp using a scalpel, and surrounding tissues were carefully cleaned to expose the skull. The primary sensory cortex (S1, ML: −3 mm, AP: −0.84 mm) was located by referring to the stereotaxic coordinates. For LSCI, a 2.0 × 2.0 mm cranial window was created using a dental drill (Strong 90 Micro Motor, Saeshin Precision, Korea) operating at approximately 10000 rpm, and a 1.4 mm steel burr was employed until the cortical vessels were visible. To prevent overheating, sterile saline was applied roughly every 15 s to the surgical area. After these procedures, the rats were allowed to recover in the cages with free access to food and water for 6 h to eliminate the effects of the anesthetics and surgery.

METHOD DETAILS

As illustrated in Figure S1A, the experimental setup consisted of several components, including modules for optical imaging, electrical signal recording, and pulsed signal generators. In this study, the ultrasound stimulation system was equipped with an immersion-type focused ultrasound transducer (V301-SU, Olympus NDT, Waltham, USA). The transducer was operated at a frequency of 500 kHz and was powered by a customized amplifier. We implemented a custom-built plexiglass acoustic collimator with a 7 mm diameter output aperture attached to the transducer to restrict the target area to the region of interest. A calibrated hydrophone (NH1000 Needle Hydrophone-1.0 mm, Precision Acoustics, UK) was employed to assess the distribution of sonic intensity with the collimator. The optical imaging modules included a 780 nm laser diode (10 mW, L780P010, Thorlabs, USA), a camera lens (Nikon AF-S VR Micro-Nikkor, 105mmf/2.8G IF-ED, Tochigi, Japan) and a CMOS camera (12bit, acA1440-220 μm, Basler, Ahrensburg, Germany), connected to computer for imaging controlling. The optical module was stabilized by holders fixed to an optical platform.

The neurovascular responses were measured by both LSCI and LFP. The principle of LSCI has been discussed in Briers and Webster.[36] In brief, the contrast value K was defined and estimated by temporal laser speckle contrast analysis (tLASCA)[37] using Equation 1 after the registration of the raw images,[38]

$$K^2 = \sigma^2 / \langle I \rangle^2, \quad \text{(Equation 1)}$$

where σ and $\langle I \rangle$ are the temporal standard deviation and the temporal average of the speckle intensity, respectively. K^2 is considered to be inversely proportional to CBF velocity,[39] therefore, the mapping of 1/ K^2 represents the spatial distribution of CBF.

The recording modules for LFP were comprised of recording, amplifying, and processing components. A tungsten microelectrode (WE50031.0A5, MicroProbe, USA) was inserted into the primary sensory cortex (S1) at a 60-degree angle to the tail direction. The recorded signals were then amplified using a pre-amplifier (PZ2, Tucker-Davis Technologies, Alachua, FL, USA) and processed with the TDT Neurophysiology Workstation (RZ2, Tucker-Davis Technologies, Alachua, FL, USA). The transducer was then positioned with a 60-degree incident angle relative to the electrode in the nose direction. A 780 nm laser diode was placed between them. To minimize the motion and vibration artifacts, optical imaging and electrical signal recording were performed on an optical table when the animals were fully anesthetized throughout the experiments.

Experimental protocols

Figure S1D shows the overview of the experimental protocols. Rats were anesthetized with isoflurane (5% initial and 1.5% maintenance) and placed in a stereotaxic frame on a heating pad to ensure body temperature of 37 ± 0.5°C. To achieve inhibition of neural activity, we administered VPA (80 mg/mL solution and 200 mg/kg body weight) via intraperitoneal (i.p.) injection in VPA group rats. At the same time, equal volumes of saline were injected in the Saline group to serve as the controls. Before the i.p. injection, a 20-s LFP-LSCI block was recorded to serve as the baseline of neurovascular activity. After 10 min of VPA or Saline i.p., another 20-s LFP-LSCI recording was performed as the before-TUS neurovascular activity. S1 region in both groups was then stimulated by TUS for 5 min, immediately after which a third 20-s block of LFP-LSCI was recorded as the after-TUS neurovascular activity.

TUS parameters

TUS's parameters in this study referred to our previous studies.[8,9] Specifically, the animals were exposed to 5-min sonication with the parameters in Figure S1C, i.e., frequency (f) = 500 kHz, inter-stimulus interval (ISI) = 4 s, sonication duration (SD) = 1 s, $spatial-peakpulse-averageintensity(I_{sppa})$ = 8.92 W/cm^2, pulse repeated frequency (PRF) = 1.5 kHz, and tone burst duration (TBD) = 0.4 ms. The ultrasound intensity was approximately 8.92 W/cm^2. As outlined in our prior study,[40] the TUS parameters described above were shown to generate negligible temperature change (less than 0.02°C). The distribution of sonic intensity with the collimator (Figure S1B) was assessed using a calibrated hydrophone.

Sodium valproate (VPA)

VPA, a salt solution of valproic acid, is a common antiepileptic drug.[41] Overdose of VPA (tpically > 100mg/kg) was reported to enhance GABA responses and block potassium and calcium channels, which would cause neural inhibition as shown in both vitro and vivo experiments.[16,21,42,43] The most marked effects of VPA could be observed in the cerebral cortex shortly (i.e., 2 to 15 min) after i.p..[21] In this study, we used 200 mg/kg VPA to achieve cortical electrical activity inhibition to control NVC. LSCI and LFP were acquired at least 10 min after the i.p. injection to ensure the VPA's effect.

LFP-LSCI recordings

As shown in Figures S1A and S1D, each LFP-LSCI block was comprised of a 20-s recording of both LFP and LSCI signals, which were synchronously controlled by the computer. The initial block termed the *Baseline* LFP-LSCI recordings, served as the reference for subsequent data analysis. The following two blocks were utilized to reflect neural activity and hemodynamic performances in rats prior and post-TUS exposure, respectively. The raw LFP signals were sampled at a rate of 3 kHz, while the optical images were acquired at 40 frames per second (fps).

Image and data processing

The image and data processing was performed in MATLAB (Ver. 2020b, MathWorks, Natick, MA, USA). Before the analysis of LFP, a notch filter was applied to the raw time traces at 50 Hz, followed by band-pass filtering between 1 Hz and 100 Hz. In cases of noisy data, the band-pass filtered LFP underwent further noise reduction through threshold de-noising and moving median filtering (temporal windows size is 1 s), enhancing the signal-to-noise ratio (SNR). We analyzed the power of LFP referring to.[44]

To improve the SNR of LSCI, a spatial 2D Gaussian filter with a standard deviation of 3 and window size of 5×5 pixels was applied to the raw speckle images. The blood flow for the initial 5 s in the Baseline block, i.e., $CBF_{baseline}$, was used as the reference for calculating mean rCBF during each of the three *Stages*.

QUANTIFICATION AND STATISTICAL ANALYSIS

Statistical analysis of neural activity and rCBF in two groups (VPA and Saline) during three *Stages* (Baseline, Post VPA/Saline(Pre-TUS), and Post-TUS) were processed in Jamovi (Ver 2.3.21). two-way ANOVA was employed to test the main effects and the interaction effect between *Stage* and *Group*. The significance level associated with these effects was determined using the Wald test. Further paired t-test was performed to describe neural activity and hemodynamic changes between *Stages* within each group. The correlation of neurovascular coupling caused by TUS was calculated by the Pearson correlation coefficient. The results are presented as the mean ± standard error of mean (*sem*).